A LINEAR DYNAMIC ANALYSIS OF VENT CONDENSATION STABILITY

C. Brennen

California Institute of Technology
Pasadena, California

ABSTRACT

Pressure suppression systems in boiling water reactors are designed to condense a large amount of steam very rapidly by injecting it into a pool of water. It transpires that such condensing flows are unstable and can lead to large oscillatory pressures on the walls of the containment system. This paper presents a theoretical model whose purpose is to attempt to understand why these flows are unstable and to extract the important parameters and frequencies pertaining to the instability. A simple linear dynamic model is constructed comprising linear transfer functions for (i) the unsteady steam flow in the vent (ii) the condensation interface and (iii) the pool hydrodynamics. The analysis demonstrates the existence of both stable and unstable regions of operation defined by several non-dimensional parameters including the ratio of the steam flow rate to the effective thermal diffusivity in the water just downstream of the condensation interface and the frictional losses in the vent. Instability frequencies are in the vicinity of the vent acoustic frequencies or the pool manometer frequency depending on the conditions. Though the qualitative dynamic behavior of the model is consistent with the experimental observations, quantitative comparison is hindered by difficulties in accurately assessing the effective thermal diffusivity in the water. Nevertheless the model provides insight into the nature of the instability.

NOMENCLATURE

A_D	Downcomer cross-sectional area.
A_I	Interface surface area.
A_P	Pool surface area.
A_S	Pool streamtube cross-sectional area.
B	$= A_I/A_D$
c	Sonic velocity of steam in downcomer.
C	Compliance of the pool.
d	Typical thermal mixing length in liquid.
f	$= f'\ell/2R$
f^*	$= fM/(1-M^2)$
f'	Downcomer friction factor.
g	Acceleration due to gravity.
G_L	A thermodynamic property
h	Mean height of interface above downcomer exit.
i	Subscript denoting position.
I	Interfacial shunt impedance
I_S	System input impedance
j	Imaginary unit
K	Interfacial impedance constant.
ℓ, ℓ_D	Downcomer length
L	Inertance of pool.
m	Mass flow rate per unit cross-sectional area of downcomer.
M	Mach number, $\bar{u}_S/c$
M^*	A thermodynamic property.
p	Pressure
R	Radius of downcomer
R^*	Radius of interfacial bubble.
$Re\{\ \}$	Denotes real part of argument.
s	Position along pool stream tube.
t	Time
$\bar{u}_L$	Mean liquid velocity.
$\bar{u}_S$	Mean steam velocity in downcomer
$[Y]$	Downcomer transfer function.
α	$K(\rho_L/\rho_V)(g^3L/4)^{\frac{1}{4}}$
γ	$(\rho_L/\rho_V)(gL/c^2)^{\frac{1}{2}}$
θ	A reduced frequency $= \Omega\ell/c(1-m^2)=\pi\omega/\sigma$
κ_1, κ_2	Eigenvalues
ξ	Inertance ratio, $\rho_L L/\rho_V \ell$
η	Thermodynamic factor $Kc^{\frac{3}{2}}/\ell^{\frac{1}{2}}$
ρ_L	Saturated liquid (water) density.
ρ_V	Saturated vapor (steam) density.
σ	Frequency ratio, Ω_D/Ω_P
τ	$\eta M\{2\pi(1-M^2)/\sigma\}^{\frac{1}{2}}$
ω	A reduced frequency $= \Omega/\Omega_P$.
Ω	Frequency
Ω_D	First downcomer acoustic frequency(half-wave) $=\pi c(1-M^2)/\ell$
Ω_P	Pool manometer frequency, $(g/L)^{\frac{1}{2}}$
$\sim$	Tilda denotes fluctuating quantity.
$-$	Overbar denotes mean flow quantity.

1. INTRODUCTION

Pressure suppression systems are incorporated into boiling water reactors in order to minimize the build up of pressure in the containment system following a hypothetical accident in which large quantities of steam escape into the "drywell" which contains the pressure vessel. They consist of vent pipes leading from the drywell to a "wetwell" partially filled with water in which the ends of the vents are submerged (Fig. 1). The intention is to condense the steam forced into the water and thus greatly reduce the final pressure within the drywell and wetwell following completion of a blowdown.

A number of difficulties with the operation of pressure suppression systems have been encountered in experiments designed to establish their performance. Some of these are associated with the early phase of a blowdown in which the gas forced into the pool is predom-

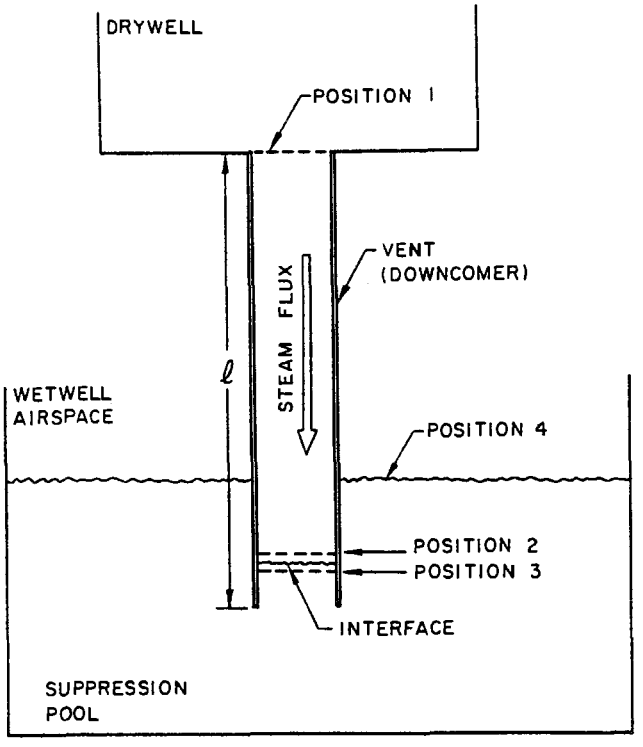

Figure 1. Schematic of a pressure suppression system in a boiling water reactor.

inantly air (originating in the drywell). However the problem considered in this report occurs later when the gas is predominantly steam. It transpires that under certain conditions the process of rapid steam condensation at an interface in the neighborhood of the vent (downcomer) exit becomes unstable, causing substantial oscillation in the position of the interface and significant pressure oscillations within the entire system. These oscillations take a number of forms. Under some conditions they are dominated by frequencies close to those of the downcomer acoustics. However, these so called "condensation oscillations" are generally less severe than the second kind which occur at lower frequencies (typically 1/4 to 2 Hz) and have been termed "chugging". The latter exhibit substantial non-linearity to the extent that each "chug" can almost be considered as a separate event which proceeds as follows. When the interface is within the vent, thermal diffusion is inhibited, the interface temperature increases and the interface is forced out of the end of the vent. Then the enhanced interfacial heat transfer leads to a rapid inward collapse of the interface. This collapse causes substantial pressure spikes within the containment which decay as the interface settles down within the vent prior to repeating the process. Though the occurrence of chugs is rather random the typical period between chugs does appear to be close to that of manometer-like oscillations of the water in the pool and vent.

There now exists a substantial quantity of data from tests designed to place operational limits on the containment loads generated by such oscillations and to investigate the governing parameters of the oscillatory phenomena (submergence, pool temperature, steam flow rate, etc.). Unfortunately much of the specific data is proprietory. There are also a number of analytical models in which chugging has been reproduced numerically (Ref. 5,7). However none of these model calculations shed much light on why and under what conditions pressure suppression systems become unstable at all. The purpose of this paper is to investigate this latter question. The emphasis here is not on any attempt to model the large amplitude, highly nonlinear processes such as chugging. Rather, we shall restrict attention to an examination of the stability of the system and to evaluating the domains within the parametric space which are stable or unstable in various frequency ranges. The procedure will therefore consist of an examination of small linear perturbations on a given steady condensing flow in a pressure suppression system.

2. DOWNCOMER AND POOL SYSTEM DYNAMICS

In this section we seek to construct a simple linear dynamic model of a pressure suppression system comprised of a single downcomer. The purpose is to investigate the linear stability or instability of assumed mean flow conditions in the system. The mean flow considered will be characterized by a mean mass flow rate of steam per unit cross-sectional area of the downcomer and a specific position of the condensation interface. If the interface is within the downcomer its position is denoted by th axial distance, h, from the interface to the exit of the interface. If the interface is outside the downcomer the situation is less readily defined and will be dealt with later.

The linear dynamics of this system will be studied by considering its response to oscillatory perturbations of frequency, Ω, imposed at the downcomer entrance. The resulting fluctuating pressures and fluctuating mass flow rates per unit downcomer cross-sectional area are denoted by

$$\mathrm{Re}\left\{\tilde{p}_i e^{j\Omega t}\right\} \quad \text{and} \quad \mathrm{Re}\left\{\tilde{m}_i e^{j\Omega t}\right\} .$$

The quantities $\tilde{p}_i$ and $\tilde{m}_i$ are considered to be small in order for the linear perturbation analysis to be valid; they are complex in general and vary with position in the system designated by the subscript i ($i = 1,2,3,4$; see below). The dynamics of the flow between any two positions, say I and J, can then be represented by a transfer matrix [Y], where

$$\begin{Bmatrix} \tilde{p}_J \\ \tilde{m}_J \end{Bmatrix} = \begin{bmatrix} Y_{11} & Y_{12} \\ Y_{21} & Y_{22} \end{bmatrix} \begin{Bmatrix} \tilde{p}_I \\ \tilde{m}_I \end{Bmatrix} \qquad (1)$$

and [Y] will in general be a function of the frequency, Ω, and the mean flow conditions in that section.

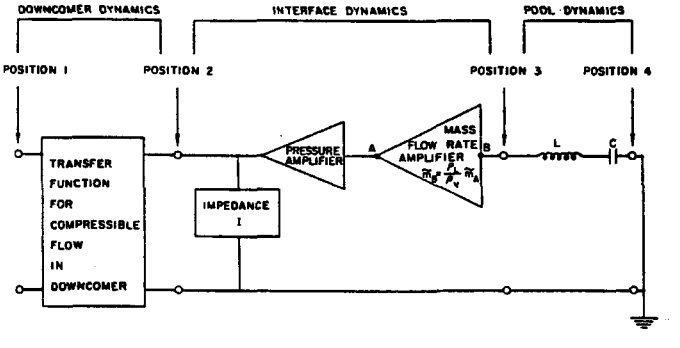

Figure 2. Breakdown of the pressure suppression system dynamics into individual components.

The dynamics of the suppression pool system will by synthesized by separating the flow into three components depicted in both Figs. 1 and 2: (i) the steam flow between the downcomer entrance (position 1) and a position immediately upstream of the condensation interface (position 2), (ii) between position 2 and position immediately downstream of the condensation interface (position 3) and (iii)between position 3 and the wetwell airspace (position 4). For convenience the dynamics of each of these three elements will be referred to as the downcomer, interface and pool dynamics respectively; transfer matrices for each will be synthesized separately and then the stability of the whole system investigated.

3. DOWNCOMER DYNAMICS

The downcomer can be modelled using the transfer matrix for compressible flow in a straight uniform pipe. Two cases are utilized herein. Firstly, in the absence of fluid friction the transfer matrix for compressible flow in a uniform pipe is (see Ref. 1)

$$\begin{aligned} Y_{11} &= (\cos\theta + jM\sin\theta)e^{j\theta M} \\ \frac{Y_{12}}{\bar{u}_S} &= -j\sin\theta e^{j\theta M}/M \\ \bar{u}_S Y_{21} &= -jM(1-M^2)\sin\theta e^{j\theta M} \\ Y_{22} &= (\cos\theta - jM\sin\theta)e^{j\theta M} \end{aligned} \qquad (2)$$

where $\bar{u}_S$ is the typical mean steam velocity in the downcomer, M the corresponding Mach number, $\bar{u}_S/c$, and θ is a dimensionless frequency $\Omega\ell_D/c(1-M^2)$; here ℓ_D is the length of the downcomer vent pipe. For simplicity we shall neglect the change in the "effective" length of the downcomer caused by changing the mean interface position and, put $\ell = \ell_D$.

When the hydraulic resistance to steam flow in the downcomer is included it is necessary to solve a quadratic dispersion relation for $\kappa = \kappa_1, \kappa_2$ as follows:

$$\kappa^2 - \kappa M(2j\theta + f^*) - j\theta(1-M^2)(j\theta + f^*) = 0 \qquad (3)$$

where f^* is the frictional term (see below). Then in terms of the average velocity along the pipe, $\bar{u}_S$, the transfer matrix is approximately given by

$$\begin{aligned} Y_{11} &= \left(\kappa_1 e^{\kappa_1} - \kappa_2 e^{\kappa_2}\right)\Big/\left(\kappa_1 - \kappa_2\right) \\ \frac{Y_{12}}{\bar{u}_S} &= -\left(j\theta + f^*\right)M^{-1}\left(e^{\kappa_1} - e^{\kappa_2}\right)\Big/\left(\kappa_1 - \kappa_2\right) \\ \bar{u}_S Y_{21} &= -j\theta M\left(1 - M^2\right)\left(e^{\kappa_1} - e^{\kappa_2}\right)\Big/\left(\kappa_1 - \kappa_2\right) \\ Y_{22} &= \left(\kappa_1 e^{\kappa_2} - \kappa_2 e^{\kappa_1}\right)\Big/\left(\kappa_1 - \kappa_2\right) \end{aligned} \qquad (4)$$

Dynamic analyses will be presented utilizing both the frictional transfer matrix and the simpler frictionless form. The frictional parameter, f^*, is given in terms of an estimated friction factor, f', for the oscillatory steam flow in the downcomer by the relation

$$f^* = \frac{fM}{(1-M^2)} \quad \text{where} \quad f = \frac{f'\ell}{2R}. \qquad (5)$$

Typical incompressible steady flow values will be used for f'.

4. INTERFACE DYNAMICS

The next element is the interface. Even for steady flows the heat transfer and two-phase flow processes occurring at the interface may be rather complex; thus it is difficult to predict the quantitative dynamics of the interface with any confidence. However, guided by a dynamic analysis of a simplified phase change boundary (Ref. 1; see also Refs. 2 and 3) we anticipate that the qualitative dynamics of the interface will be as indicated in Fig. 2. The mass flow rate amplification is such that $\tilde{m}_B = \tilde{m}_A(\rho_L/\rho_V)$ where ρ_L/ρ_V is the ratio of saturated liquid to saturated vapor density at the mean interface temperature or pressure (see Ref. 1, Fig. 5). The impedence, I, to ground is given by

$$I = 1/(1+j)\left(\frac{\Omega}{2}\right)^{\frac{1}{2}}K \qquad (6)$$

where K depends on (i) the ratio of the actual interface area, A_I, to the cross-sectional area of the downcomer, A_D, denoted by $B = A_I/A_D$ (this could be quite large if the actual interface is convoluted and bubbly); (ii) on the degree of enhancement of the heat transfer in the neighborhood of the interface due to turbulent mixing. In the absence of such turbulent mixing the value of K is given by BM^* where M^* is a function only of the mean interface temperature and was plotted in units of $\sec^{\frac{3}{2}}/m$ for different fluids in Ref. 1. If, on the other hand the heat diffusion is dominated by turbulence rather than fluid conductivity the value of M^* is better estimated as $\rho_L G_L(\bar{u}_L d)^{\frac{1}{2}}$ where $\bar{u}_L$ is the typical mean flow velocity of the liquid $(\approx\bar{u}_S\rho_V/\rho_L)$, d is the typical mixing length and G_L is another thermodynamic quantity which is also presented in Ref. 1. It should be stressed that the principal uncertainty in the model of the interfacial dynamics is the effective thermal diffusivity of the liquid which determines K and therefore the impedance I; there is clearly a need for experiments to evaluate these quantities.

The pressure amplifier has an amplification factor of

$$1 + 2\bar{u}_S K(1+j)\left(\frac{\Omega}{2}\right)^{\frac{1}{2}}.$$

It transpires that this amplification is essentially unity and the effect of the pressure amplifier on the system response is very small except at downcomer Mach numbers approaching unity and/or at very high frequencies (see Ref. 1).

5. POOL DYNAMICS

It remains to model the third component, the suppression pool itself. Like any pool or manometer its dynamics are comprised of inertial and compliant elements, L and C, in series as indicated in Fig. 2. Note that if the interface were at constant pressure (i.e. grounded) the subsequent natural frequency of the pool alone, Ω_p, would be $1/(LC)^{\frac{1}{2}}$. The inertive element,

L, represents the pressure difference due to the acceleration of the fluid between positions 3 and 4; the compliant element, C, represents the pressure difference caused by the quasistatic displacement of fluid in the presence of gravity. Each stream-tube beginning just downstream of the interface and ending at the free surface of the pool has an inertance based on mass flow rate per unit downcomer area given by

$$L = A_D \int \frac{ds}{A_S(s)} \quad . \tag{7}$$

If the pool free surface area is large compared with A_D the major contributions to L arise from the liquid column within the downcomer (if any) and from the expanding source-like flow at the vent exit. When the interface is within the downcomer (Fig. 3a) these two

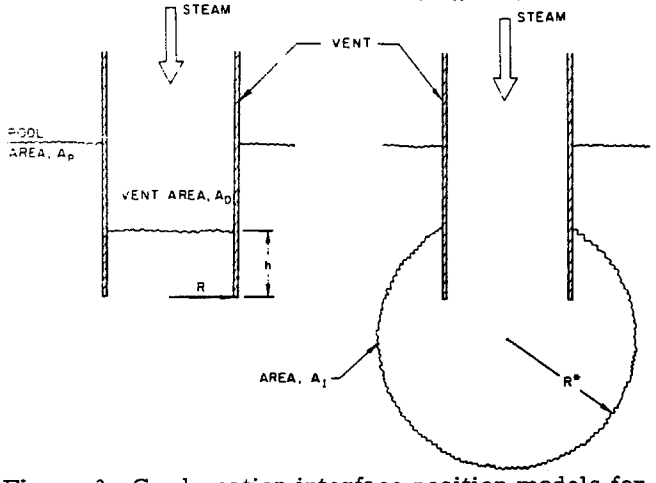

Figure 3. Condensation interface position models for the analysis of the pool dynamics (a)mean position of interface inside the vent (b)mean position of interface external to the vent.

contributions can be estimated to be approximately h and R respectively. Furthermore, since a downward displacement δh in the interface position under these circumstances simply leads to an increased pressure difference between positions 3 and 4 of $\rho_L g \delta h$ the compliance, C, based on mass flow rates per unit downcomer is 1/g. Thus in the simpler case in which the interface is within the vent (and pool surface area $\gg A_D$)

$$L \approx h + R \; ; \; C \approx \frac{1}{g} \quad . \tag{8}$$

Sensible estimates in the case in which the interface is outside the downcomer exit are less readily obtained since they depend upon the form and position of the interface. As a first approximation one could assume a spherical bubble interface (Fig. 3b) of surface area, A_I. Since the inertance surrounding a spherical bubble of radius R^* is $A_D/4\pi R^*$ the inertance of the pool would then be $L = A_D/(4\pi A_I)^{\frac{1}{2}}$. The pool compliance, C, for this case is more uncertain since it depends upon the extent to which the center of the volume of the bubble moves up and down during oscillatory contraction and expansion. The calculations would proceed as follows. Suppose that during a short time interval within a cycle of oscillation the volume of the bubble increased by δV. If the center of the volume is displaced downward by a distance δh then the net increase in hydrostatic pressure experienced on the average by the bubble is

$$\rho_L g(\delta h + \frac{\delta V}{A_P})$$

It follows that the pool compliance is

$$C = 1/g \left\{ \frac{A_D \delta h}{\delta V} + \frac{A_D}{A_p} \right\} \quad . \tag{9}$$

To correlate this with the value of 1/g when the interface is within the downcomer note that under those circumstances $A_D \delta h/\delta V = 1$ and the small factor A_D/A_p could be neglected. However when the interface is outside the downcomer is quite possible that $A_D \delta h/\delta V$ may become very much less than unity. Thus the compliance can be very much larger than in the internal interface situation. The most convenient way in which to generalize this effect upon the compliance is to regard the quantity g as the acceleration due to gravity when the interface is within the vent and as some "effective" value less than the acceleration due to gravity for the case in which the interface is external to the vent.

In general the pool dynamics should also include some frictional resistance relevant to the water flow in the downcomer and at its exit. This has been omitted in the present model since the dominant frictional effect will be that of the steam in the downcomer.

In summary, the inertance as represented by L will increase and the compliance as represented by g^{-1} will decrease as the interface moves from a position outside the vent to one within the vent. Hence the trend in the "natural frequency" of pool, $\Omega_p = (g/L)^{\frac{1}{2}}$, may not be a simple one.

6. SYSTEM RESPONSE

The input impedance, I_s of the pressure suppression system modelled in Fig. 2 is

$$I_S = \frac{\tilde{m}_1}{\tilde{p}_1}$$

$$= \frac{\begin{bmatrix} Y_{11}\{1+(j-1)\alpha\omega^{\frac{3}{2}}(1-\omega^{-2})+(1+j)\omega^{\frac{1}{2}}\tau\} \\ -j\omega\gamma(Y_{21}c)(1-\omega^{-2}) \end{bmatrix}}{\begin{bmatrix} j\omega\alpha Y_{22}(1-\omega^{-2}) \\ -Y_{12}c^{-1}\{1+(j-1)\alpha\omega^{\frac{3}{2}}(1-\omega^{-2})+(1+j)\omega^{\frac{1}{2}}\tau\} \end{bmatrix}} \tag{10}$$

where ω is a convenient reduced frequency given by Ω/Ω_p. Furthermore if Ω_D denotes the acoustic resonant frequency of the downcomer (the half-wave frequency in radians/sec), i.e.

$$\Omega_D = \pi c(1 - M^2)/\ell \tag{11}$$

it follows that in the expressions (2), (4) for the Y matrix elements $\theta = \pi\omega/\sigma$ where σ is the ratio Ω_D/Ω_p.

The primary non-dimensional parameters appearing in the above expression for the input impedance are (i) $\sigma = \Omega_D/\Omega_p$ (ii) the Mach number, M, which is the non-dimensional form of the mean flow rate, (iii) the downcomer friction parameter, f, (iv) the parameter, α, and (v) the parameter, γ, given respectively by

$$\alpha = K\left(\frac{\rho_L}{\rho_V}\right)\left(\frac{g^3 L}{4}\right)^{\frac{1}{4}} \tag{12}$$

$$\gamma = \left(\frac{\rho_L}{\rho_V}\right)\left(\frac{gL}{c^2}\right)^{\frac{1}{2}} \tag{13}$$

Though α and γ appear most naturally in the expression (10) for the input impedance they are not the most convenient parameters from an experimental point of view. Hence we define two alternative parameters which, in addition to σ, M and f, define the parametric space, namely

$$\xi = \frac{\rho_L L}{\rho_V \ell} \tag{14}$$

and

$$\eta = \frac{Kc^{\frac{3}{2}}}{\ell^{\frac{1}{2}}} \tag{15}$$

The parameter, ξ, is the only one in the system $(\sigma, M, \xi, \eta, f)$ in which the density ratio appears explicitly. For a given geometry it therefore varies with interface temperature and position (as manifest by L). It will be termed the "inertance ratio" because it clearly is a measure of the relative inertances of the pool water and the downcomer steam. On the other hand, the thermodynamic factor, η, is the only one in the system $(\sigma, M, \xi, \eta, f)$ in which K appears. It does not depend explicitly on the interface position. However in practical circumstances the degree of water mixing and the effective thermal diffusivity in the water may well be a strong function of the interface position. This in turn effects K and thus, implicitly, the factor, η. The system response (that is to say $c\,I_S$) is then a function only of the dimensionless parameters $\omega, \sigma, M, \xi, \eta$, and f. (Relations for α, γ and τ in terms of these parameters are listed in the nomenclature)

The next step is to determine the stability of the system by examining the sign of the resistive or real part of the input impedance. If this is positive the system dissipates energy and is stable; if it is negative the system is inherently unstable. This can be done most readily by numerical evaluation of $c\,I_S$ over a range of frequencies, ω, given values of σ, M, ξ, η, and f. Results of this kind are presented later. Though it is possible to continue analytic manipulation of the impedance, the algebra is exceedingly lengthy in the most general case and its presentation is of little value. It is however of some value to perform further algebraic inspection of the results in the simpler case in which the downcomer friction is neglected. Then the impedance can be written as

$$I_s = \frac{\left[(\cos\sigma + jM\sin\sigma)\{1+(j-1)\alpha\omega^{\frac{3}{2}}(1-\omega^{-2})+(j+1)\omega^{\frac{1}{2}}\tau\}\right] - \omega\gamma(1-M^2)(1-\omega^{-2})\sin\sigma}{c\left[j\omega\alpha(1-\omega^{-2})(\cos\sigma - jM\sin\sigma) + j\sin\sigma\{1+(j-1)\alpha\omega^{\frac{3}{2}}(1-\omega^{-2})+(j+1)\omega^{\frac{1}{2}}\tau\}\right]} \tag{16}$$

Rationalizing this expression it is observed that the sign of the real part of the input impedance is the same as the sign of the quantity, Γ, where if the τ terms are neglected (their effect is negligible except as M approaches unity):

$$\Gamma = \alpha\gamma\omega^{\frac{5}{2}}(1-\omega^{-2})^2\{1-2M^2\sin^2\theta\} + M\sin\theta\left[\begin{array}{l}\sin\theta + 2\omega\gamma(1-\omega^{-2})\{1-\alpha\omega^{\frac{3}{2}}(1-\omega^{-2})\}\cos\theta \\ -2\alpha\omega^{\frac{3}{2}}(1-\omega^{-2})\sin\theta + 2\alpha^2\omega^3(1-\omega^{-2})\sin\theta \\ -\omega^2\gamma^2(1-\omega^{-2})^2(1-M^2)\sin\theta\end{array}\right] \tag{17}$$

where it should be recalled that $\theta = \pi\omega/\sigma$. Thus the system without downcomer friction is stable if $\Gamma > 0$. and unstable when $\Gamma < 0$. The last expression is of value in interpreting some features of the numerical results which follow.

7. STABILITY CALCULATIONS

The case of a frictionless downcomer (f=0) will be studied first and the effects of $f \neq 0$ examined subsequently. Typical values of the input resistance (or real part of the impedance) as a function of the reduced frequency, ω, are presented in Fig. 4. The case shown is for an inertance ratio, $\xi = 1.5$, a frequency

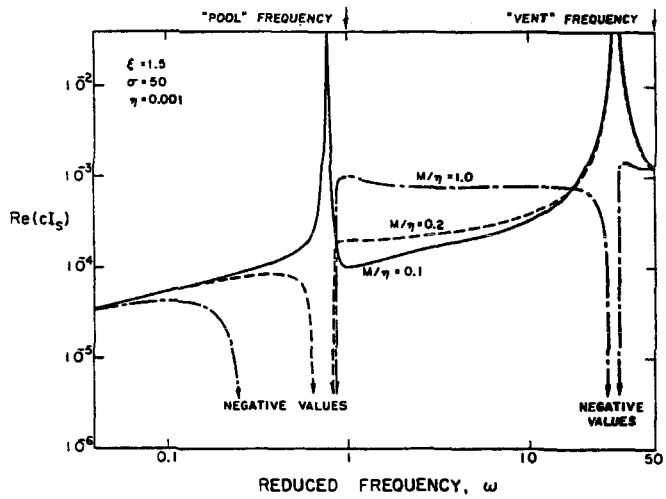

Figure 4. The real part of cI_S where I_S is the system impedance plotted against reduced frequency, $\omega = \Omega_D$ for $\xi = 1.5$, $\sigma = 50$, f=0, $\eta = 0.001$ and various M/η as indicated.

ratio, $\sigma = 50$ and a value of $\eta = 0.001$; results are plotted for three different Mach numbers though for reasons which will become clear these are designated by the values of $M/\eta = 0.1$, 0.2 and 1.0.

This and other such plots for given ξ, σ and η exhibit the following behavior. Below a certain value of the Mach number the resistance is positive and the system is stable for all frequencies. There are peaks

in this resistance, the first of which occurs at a frequency somewhat below the "pool" frequency; the second occurs at a frequency somewhat less than the "vent" acoustic frequency. There is also a succession of further peaks at higher frequencies. This behavior is exemplified by the curve for $M/\eta = 0.1$.

As the Mach number is increased a value is reached at which the first peak becomes a trough in which negative values of the resistance are exhibited. Thus the system has become unstable over this small range of frequencies. The value of M/η at which this occurs (or, more specifically, at which the resistance at the minimum in the first trough is zero) is termed the first critical and has a value of 0.156 in the example shown. At this value of M/η the remaining peaks at higher frequencies remain positive. Hence in the absence of vent friction the system first becomes unstable at a frequency somewhat below the "pool" frequency.

As the Mach number is further increased (from $M/\eta = 0.2$ to 1.0 in the example shown) the second peak becomes a trough at a second critical value of M/η (0.97 in the example). The system has then become unstable in a second range of frequencies somewhat below the vent acoustic frequency. Further increase in M/η continues this domino effect in which successive peaks become troughs.

The reason for quoting critical values of M/η is that providing $M<<1$ (as it is in most of the pressure suppression systems) then the critical conditions are not dependent on M and η separately but involve only the ratio M/η . This result can be deduced from the expression (17) for Γ; when $M<<1$, M only occurs in front of the square bracket and α (or η) only occurs as a linear multiplier in the first term of the right hand side. It follows that the condition for $\Gamma = 0$ does not involve M and η separately but only the ratio M/η .

The above sequence of events were described in the context of an increasing flow rate (M) for a given degree of mixing in the pool (given η). However, it may be of crucial importance to realize that the same sequence of events would occur for a given flow rate (given M) if the degree of mixing or effective thermal diffusivity in the pool were decreased. Such may be the case if the mean position of the interface shrinks into the downcomer.

First and second critical values of M/η and the frequencies, ω, at which they occur are displayed in Figs. 7, 8, 9 and 10 as functions of the inertance ratio, ξ, for various values of the frequency ratio, σ, and the vent friction parameter, f.

The effects of vent friction on the frequency response are illustrated in Figs. 5 and 6 and are rather interesting. As anticipated vent friction is stabilizing but the relative effects on the first and second criticals are particularly noteworthy. Figure 5 shows that at a value of M/η between the first and second critical for $f = 0$ the addition of a small amount of vent friction ($f = 0.02$) is sufficient to stabilize the system. The first critical value of M/η is therefore increased as shown by the dashed lines in Fig. 7. This change is very much a function of both ξ and σ . The effect of a given value of f is much larger the greater the frequency ratio, σ . Furthermore, below a certain inertance ratio, ξ, the critical value of M/η for non-zero friction departs radically from the frictionless case and increases rapidly with decreasing ξ as indicated by the dashed lines in Fig. 7. Indeed the value

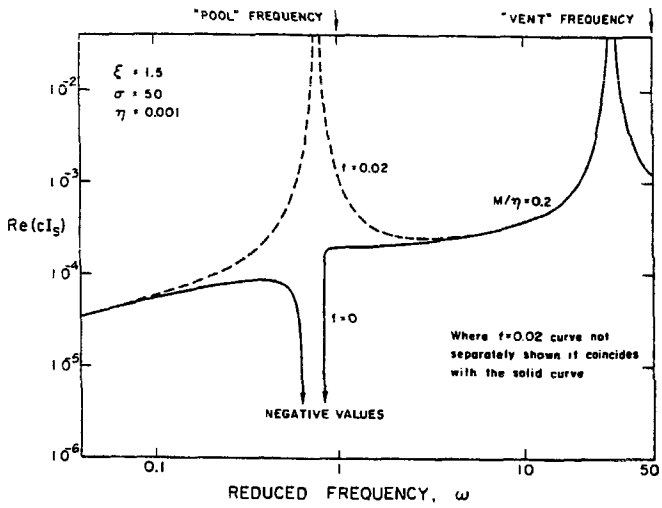

Figure 5. The real part of cI_S where I_S is the system impedance plotted against reduced frequency for $\xi = 1.5$, $\sigma = 50$, $\eta = 0.001$, $M/\eta = 0.2$ and two values of the downcomer friction parameter as indicated.

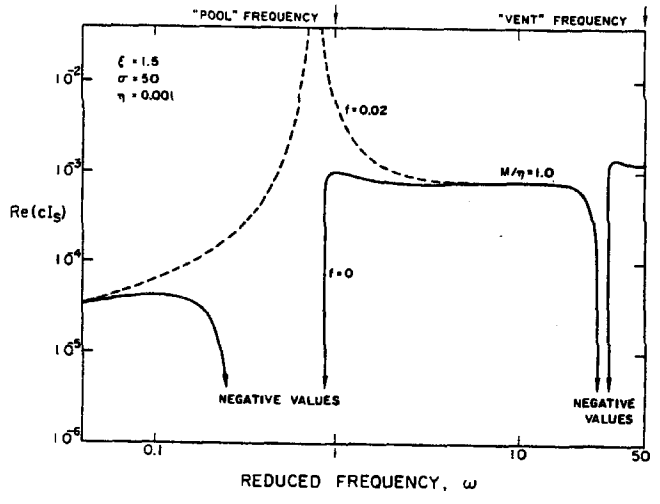

Figure 6. The real part of cI_S where I_S is the system impedance plotted against reduced frequency for $\xi = 1.5$, $\sigma = 50$, $\eta = 0.001$, $M/\eta = 1.0$ and two values of the downcomer friction parameter as indicated.

of the "first" critical M/η can become larger than the value of the "second" critical for certain choices of ξ, σ and f. The result is the interesting possibility illustrated in Fig. 6. The frictionless system $\xi = 1.5$, $\sigma = 50$, $M/\eta = 1.0$ is unstable in both the first and second critical frequency ranges. The addition of friction stabilizes the "first" critical much more effectively and, if $f = 0.02$, the result is a system which is unstable in the second, higher critical frequency range but not at the first critical lower frequency range.

Furthermore, practical values of f would normally be significantly larger than 0.02; a more representative situation is presented in Fig. 8 for a value of $f = 0.5$. Here the reversal described at the end of the last paragraph has become widespread and the lower frequency "first critical" occurs at higher values of M/η than the higher frequency "second critical" (at least for $\sigma > 5$). Figure 8 also demonstrates that

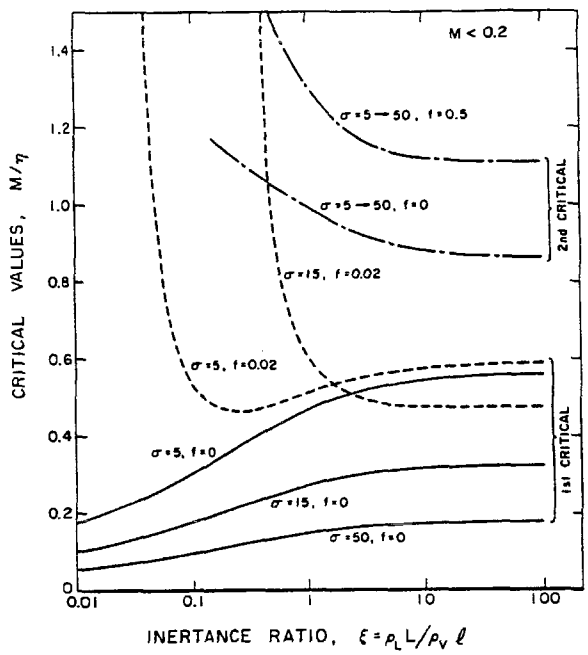

Figure 7. The first and second critical values of M/η as functions of the inertance ratio, ξ, and various σ and f as shown. The results are valid for M (and thus η) such that M is less than about 0.2.

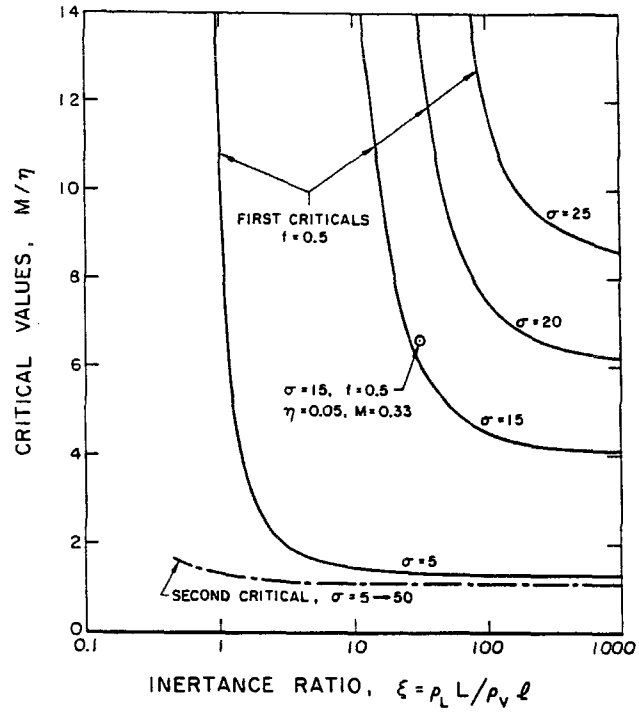

Figure 8. The first and second critical values of M/η as functions of the inertance ratio, ξ, for a friction parameter f = 0.5 and various σ. One point (⊙) is shown for η = 0.05, M=0.33 to indicate the nature of the departure of the results at high Mach number from the curves shown.

either a decrease in the frequency ratio, σ, or an increase in the inertance ratio could cause destabilization of a system with reasonable amounts of downcomer friction.

Finally, a comment regarding the separate effect of downcomer Mach number, M, on the results of Figs. 7, 8, 9 and 10 is necessary. Most of this data was obtained for fixed values of η of the order of 0.001 or 0.01; that is to say for $M << 1$. However, virtually no change was observed in the results as η was increased (equivalent to increasing M) until Mach numbers of the order of 0.3 or so were encountered. Thus, the data presented is considered accurate for all Mach numbers less than about 0.2. Above this value the trend was toward increased stabilization; one point at a Mach number of 0.33 is included in Fig. 8 to demonstrate this.

8. CONDENSATION OSCILLATIONS AND CHUGGING

Much data has now been gathered on the operation of pressure suppression systems in boiling water reactors; investigations on both large and small scales have been carried out in Germany, (Ref. 4, 6), Sweden, U.S.A. and elsewhere. Most of this information is in the form of transient blowdowns in which the parameters utilized in the above analysis are varying with time. Following the air blowdown phase which is not being studied here the blowdown traverses some line within the parametric space M, σ, ξ, η (assuming that if f is relatively constant). Our objective here will be to examine the nature of a typical traverse and to try to understand the observed phenomena (see section 1) in the light of the analytical results of the last section.

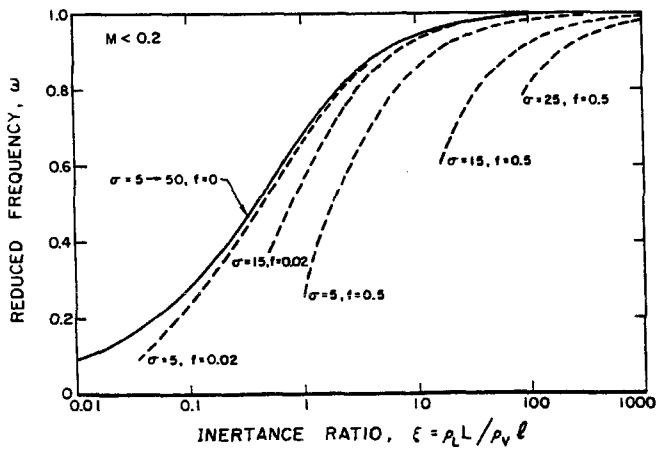

Figure 9. The first critical frequency plotted against the inertance ratio, ξ, for various σ, f and for Mach numbers less than about 0.2.

Toward this end it is instructive to choose numerical values from a typical blowdown test facility. Taking a 25m. downcomer (ℓ=25m.) with a diameter of 0.5m. and a reasonable friction factor, f', of 0.01 it follows that $f \approx 0.5$ and thus the discussion will center on Fig. 8. For a typical downcomer steam sonic velocity of 500m/sec the Mach number M will decrease from a maximum of about 0.1 to zero as the steam blowdown proceeds (this corresponds to a typical steam flux of about 30 kg/m^{2}sec). Also for a typical